48th International Symposium of Applied Aerodynamics
Saint-Louis, 25-27 March 2013

Study of a Flexible UAV Proprotor

48th APPLIED AERODYNAMICS SYMPOSIUM
Saint-Louis, FRANCE, 25-27 MARCH 2013
Fazila MOHD-ZAWAWI[(1)], Sebastien PROTHIN[(2)], Peng LV[(3)],
Emmanuel BENARD[(4)], Jean-Marc MOSCHETTA[(5)], Joseph MORLIER[(6)]
[(1)-(5)] Université de Toulouse, ISAE, 10 av. Edouard Belin - BP 54032 - 31055 Toulouse Cedex 4, France
[(6)]Université de Toulouse, ICA, ISAE/INSA/UPS/ENSTIMAC, 10 av. Edouard Belin - BP 54032 - 31055 Toulouse Cedex 4, France
Corresponding email: fazila.mohd-zawawi@isae.fr

Abstract: This paper is concerned with the evaluation of design techniques, both for the propulsive performance and for the structural behavior of a composite flexible proprotor. A numerical model was developed using a combination of aerodynamic model based on Blade Element Momentum Theory (BEMT), and structural model based on anisotropic beam finite element, in order to evaluate the coupled structural and the aerodynamic characteristics of the deformable proprotor blade. The numerical model was then validated by means of static performance measurements and shape reconstruction from Laser Distance Sensor (LDS) outputs. From the validation results of both aerodynamic and structural model, it can be concluded that the numerical approach developed by the authors is valid as a reliable tool for designing and analyzing the UAV-sized proprotor made of composite material. The proposed experiment technique is also capable of providing a predictive and reliable data in blade geometry and performance for rotor modes.

1. INTRODUCTION

Tilt-body Micro Air Vehicle (MAV) has been developed to be multifunctional in order to offer a wide range of services. It can fly in both of hover and forward flight. In 2008, Shkarayev S. and Moschetta J.M. introduced the efforts on the aerodynamic design of a tilt-body MAV named mini-Vertigo, which had a tilt-body configuration [1]. The wind tunnel measurements were conducted for a motor, a wing, and an arrangement of a wing with a motor. The results were realized in the design of a Tilt-body MAV prototype which was successfully tested in flight. Tilt-body MAV attracts growing interest as they offer great versatility in the field of urban reconnaissance. A key issue to solve for optimal operation is the problem that a stiff proprotor cannot operate efficiently for both hover and forward flights. Mark W. Nixon proposed a passive blade twist control method for conventional proprotor of tilt-rotor aircraft using extension twist coupling [2]. Unfortunately most of large scale adaptation techniques are not transferrable to small scale rotor based MAV. Finally, the combination of passive twist control and active pitch control enhanced the proprotor performance. In the present study a passive twist control is considered as a potential way to improve the overall flight efficiency of MAV proprotor. The proprotor blade made of composite material is preferred to be used. It is due to their potential benefits such as aeroelastic tailoring, ability to manufacture more refined aerodynamic designs for platform/airfoil geometries and significant enhancements in fatigue performance and damage tolerance of the blade. Additionally, the difference in rotor speeds in hover and forward flight modes may cause a change in the blade centrifugal forces so that extension-twist structural coupling can be optimized for a given proprotor blade for convertible air vehicles. Hence, this paper is aimed at developing an evaluation of design techniques of a composite flexible proprotor.

2. NUMERICAL MODEL

2.1. Aerodynamic Model (FPROP)

The aerodynamic model based on BEMT is used as a tool to compute the aerodynamic loadings in terms of lift force, drag force and pitching moment around quarter of the chord distributed in spanwise. The quasi-steady aerodynamic loading is calculated using a two-dimensional aerodynamic theory in a strip-manner. In the aerodynamic modeling for forward flight case, the BEMT proposed by Adkins is adapted, meanwhile; a classical BEMT is used for hover case. The detailed equations used for both are described in [3] and [4], respectively. In this model, the flow angle is iteratively computed until the convergence criteria are reached. This iterative analysis procedure determines the characteristics of a given proprotor (C_T, C_P) and its corresponding performance ($\eta_{proprotor}$, FM). The radial and axial interference factors (a, a'), and Reynolds number (Re) depending on the operating condition are also iteratively computed in the analysis process.

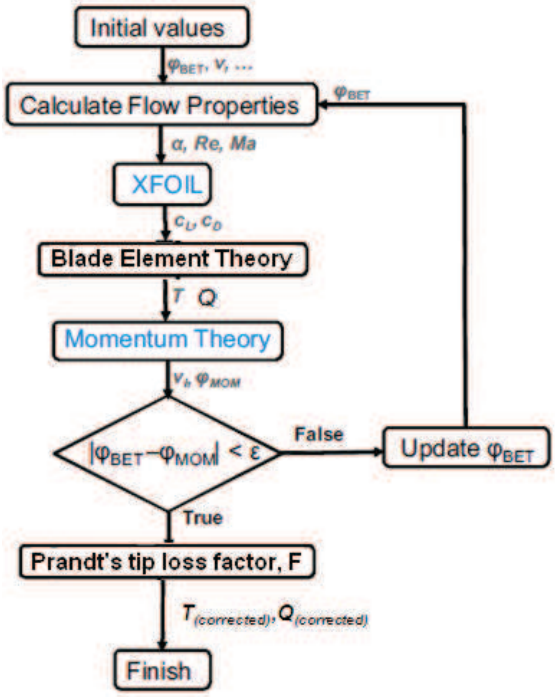

Figure 1. BEMT procedure in FPROP

In the classical approach of low order proprotor analysis, different assumptions are used, i.e lift polar is a linear function, in order to obtain a closed loop solution or even to quickly converge the iterative process. Hence, in order to consider non-linear airfoil characteristics prevalent in low Reynolds number regime (Re<70,000), XFOIL, an airfoil design and analysis code developed by Drela [5] was integrated into the design iterative process to eliminate this assumption as well as to precisely compute the aerodynamic coefficients. The airfoil sensitivity to the turbulence level and Reynolds number variation was eliminated by using flat plate [6] as a blade profile for analysis in this study. Flat plate profile also promises better performance than other airfoils in MAVs Reynolds number regime [7]. In this respect, the n_{crit} parameter, used to define the turbulence level in XFOIL, can be set as 0.1 for both flight modes. The developed iterative process of analysis procedures using BEMT method was validated with the QPROP and the experimental measurement [8]. The BEMT procedure of FPROP is shown as a block diagram in Fig. 1. The result validation of BEMT for hover and forward flight cases in terms of thrust and torque are shown in Fig. 2 and Fig. 3, respectively.

A 2-bladed rotor with rectangular planform (R=0.1m, c=0.02m), flat plate blade profile with thickness t/c=2.5% and blade pitch of 25° was used in the aerodynamic model validation for a case without inflow (hover case). Meanwhile, the propeller APC 8x6 was used to validate the FPROP for forward flight case. The inflow velocity was 16m/s.

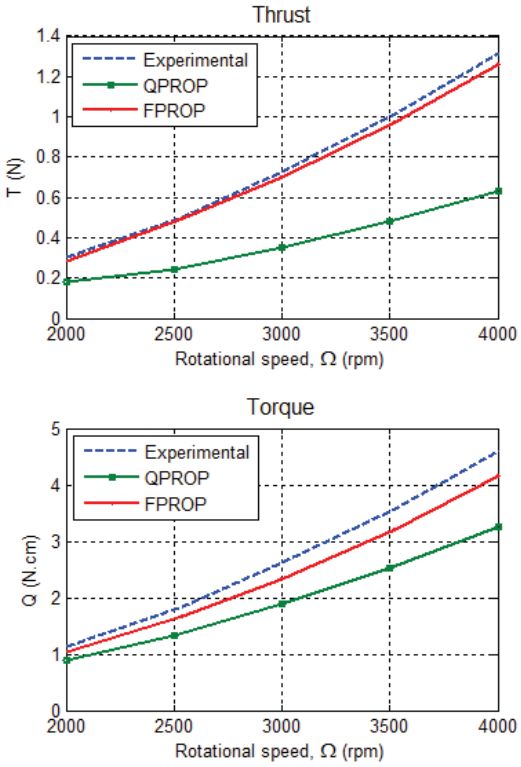

Figure 2. Comparison of BEMT simulation and the corresponding measurements for hover case (V=0)

From the validation result, it is found that the developed BEMT method with the integration of XFOIL shows better agreement with the experimental measurement compared to QPROP. QPROP, a propeller analysis tool with simplification of linear lift polar, showed unacceptable results due to its incapability to predict aerodynamic coefficients at post-stall angle of attacks. A slight increase in torque observed in the experimental result is can be due to the heavy material (aluminium) used in the blade.

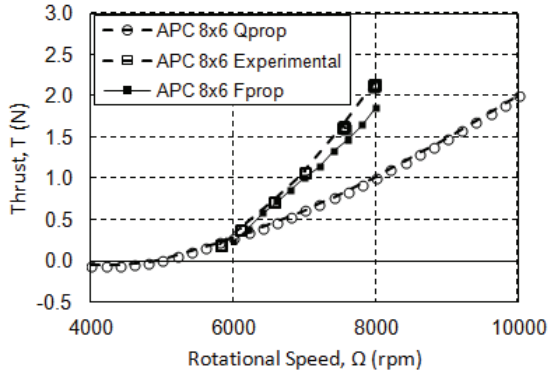

(a) Thrust

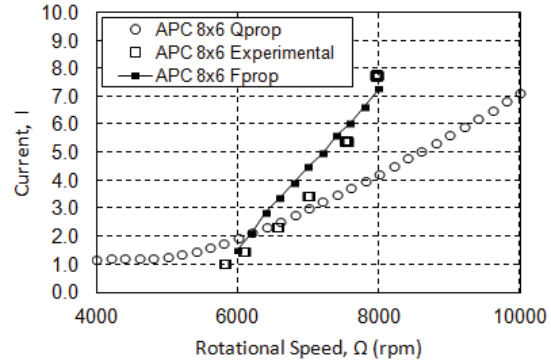

(b) Torque

Figure 3. Comparison of BEMT simulation and the corresponding measurements with inflow (V=16m/s)

2.2. Structural Model (FBEAM)

The structural analysis is based upon the use of anisotropic beam finite element model to determine the blade deflections during operation. The FBEAM consists of an integrated set of programs, which perform a two-dimensional cross-sectional analysis of the blade, followed by a one-dimensional finite element of a proprotor blade. A global coordinate system, shown in Fig. 4 is used for the description of the blade geometry and the calculation of the loads. This is a right-handed Cartesian coordinates system where; the Y-axis is co-linear with the proprotor rotation axis and its positive in the direction of flight. The Z-axis is in the plane of rotation and points towards the blade tip. The X-axis is chordwise direction where the feathering axis is referred to. In this study, feathering axis was set at quarter-chord.

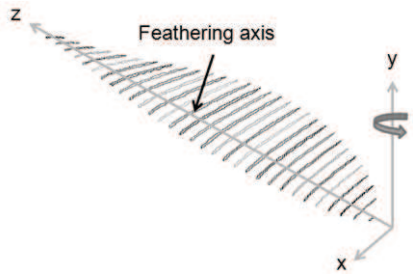

Figure 4. Global coordinate system of the blade

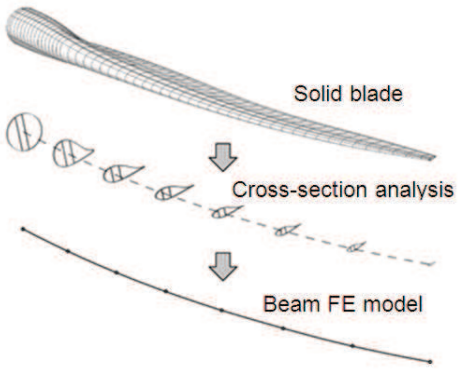

Figure 5.Finite element beam model and cross-sectional analysis

BECAS [9], a cross-sectional analysis tool which is developed at Denmark Technical University (DTU) was incorporated in this structural analysis program. The motivation of employing BECAS in this two-step structural model is due to the fact that BECAS has ability to determine the cross section stiffness properties while accounting for all the geometrical and material induced couplings. These properties are also consequently utilized in the development of beam models to accurately predict the response of proprotor blades with complex geometries and made of advanced materials. A linear elastic beam theory is assumed in the cross section analysis. The linear relation between the cross section that generalized forces T and moments M (Figure 6(a)) and the resulting strains τ and curvatures κ (Figure 6(b)) is

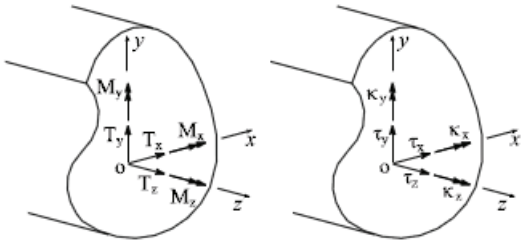

Figure 6. Cross section coordinate system, forces and moments (a) and corresponding strains and curvatures (b)

written in a stiffness form as follows:

$$\begin{bmatrix} T_x \\ T_y \\ T_z \\ M_x \\ M_y \\ M_z \end{bmatrix} = \begin{bmatrix} S_{11} & S_{12} & S_{13} & S_{14} & S_{15} & S_{16} \\ S_{21} & S_{22} & S_{23} & S_{24} & S_{25} & S_{26} \\ S_{31} & S_{32} & S_{33} & S_{34} & S_{35} & S_{36} \\ S_{41} & S_{42} & S_{43} & S_{44} & S_{45} & S_{46} \\ S_{51} & S_{52} & S_{53} & S_{54} & S_{55} & S_{56} \\ S_{61} & S_{62} & S_{63} & S_{64} & S_{65} & S_{66} \end{bmatrix} \begin{bmatrix} \tau_x \\ \tau_y \\ \tau_z \\ \kappa_x \\ \kappa_y \\ \kappa_z \end{bmatrix}$$

where S_{ij} is the sectional stiffness matrix. Using the sectional stiffness matrix and mass matrix obtained in BECAS, the elemental stiffness matrix and mass matrix are evaluated. Elastic energy and kinetic energy of the beam element are considered in order to compute the elemental properties. The final form of elastic energy and kinetic energy are written in Eq. 2.1 and Eq 2.2, respectively.

$$K_e = \int_0^L B^T.S.B.dz \tag{2.1}$$

$$M_e = \int_0^L N^T.M_s.N.dz \tag{2.2}$$

where M_s sectional mass matrix, B is the strain-displacement matrix and N is the polynomial matrix. The details equation used in these relationships are described in [10]. Global stiffness of the blade is obtained through spanwise integration. As for the one-dimensional finite element, the classical Timoshenko beam theory is used for considering finite element analysis. Static equilibrium equations are solved with the geometric boundary conditions in order to compute the shape function. With the obtained shape function, the principle of virtual displacements is used to derive the elemental stiffness. And for the purpose of integration, a Gauss quadrature is used where for this study, four-noded one-dimensional elements were chosen.

The load caused by the body forces generated by the central acceleration field, including centrifugal effects are included in the structural model. The stretching induced by the centrifugal inertia force due to the rotational motion causes the increment of the bending stiffness of the structure which naturally results in the variation of natural frequencies and mode shapes.

For structural model validation, a static analysis on a rectangular planform with dimension (190.5mmx12.7mmx3.175mm) was performed. Graphite-epoxy with material properties E_{11}=129GPa, E_{22}=9.4GPa, E_{33}=9.4GPa, G_{12}=5.16GPa, G_{13}=4.3GPa, G23=2.54GPa, vu=0.3 and ρ=1550kg/m^{3}was used. The ply anglewith respect to pitch axis was 30°. The result obtained in FBEAM was validated by commercial structural analysis program namely MSc. Nastran and the validation result is illustrated in Fig. 7.

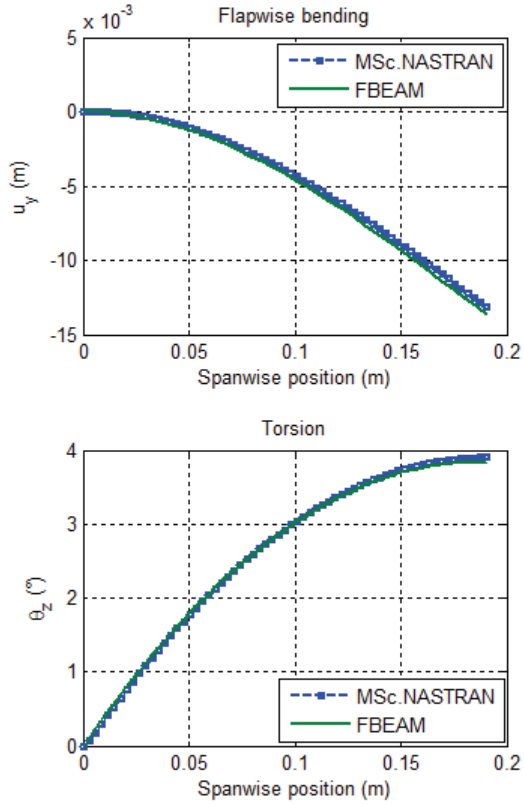

Figure 7. FBEAM validation by MSc. NASTRAN

Several simulations were carried out to observe the operating condition and fiber orientation effect on blade deformations which later will be used for prediction in the design process. Fig. 8 illustrates the effect of using anisotropic material on the bending and torsion deformations. Fig. 9 demonstrates the deformations at different RPM.

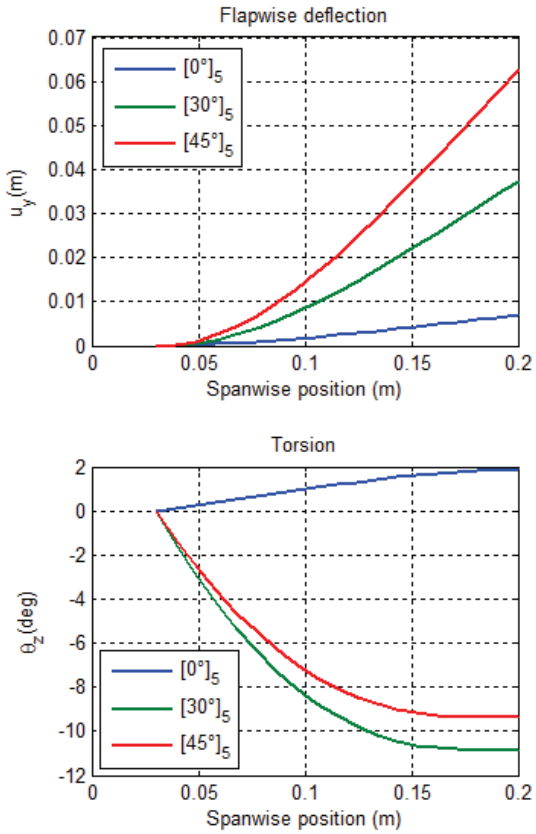

Figure 8.Effect of fiber orientation on blade deformations (β=15°, RPM=1500)

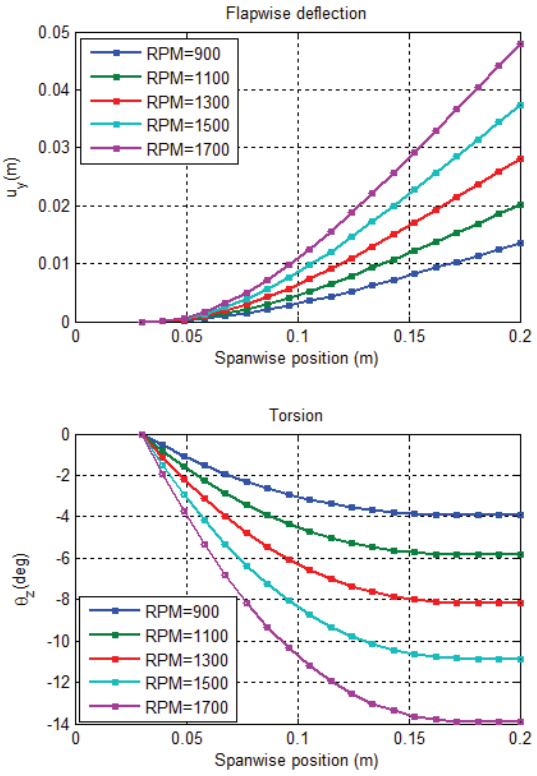

Figure 9. Blade deformations at different RPM (Fiber angle=45°)

From the result in Fig. 8, it is found that the load in flapwise direction not only produces flapwise defelction but also torsion.

2.3. Coupled-aero-structure (FAE)

In order to compute the blade deformation under aerodynamic loadings, the coupled-aero-structure model is developed. The coupled aero-structure of the proprotor combines the aerodynamic and structural analysis models. To begin with, the basic geometry (zero deflections) is assumed. Then the FBEAM structural model calculates the blade deformations under centrifugal loads. The deformed blade shape is used to update the aerodynamic model. The quasi-steady aerodynamic loads are computed for the update geometry, using the 2D aerodynamic theory based on stripwise manner model as described in section 2.1. The aerodynamic loads are transferred to the beam FE nodes as concentrated forces. A new structural analysis is performed to calculate the deformed shape of the blade under the influence of aerodynamic and centrifugal loads. The variation of the blade twist angle along the blade is monitored for convergence. The aero-structural interaction is repeated until equilibrium between deformation and loadings is achieved. After convergence the proprotor performance characteristics are computed. The approach described above was applied to the constant chord untwisted 2-bladed system for UAV-sized proprotor made of laminate composite. The deflection results in two basic modes of deformation; spanwise bending and torsion. The effects of camber changes are not included in this study due to limitation in the modeling. Iteration 1 denotes the deflection due to centrifugal loads only and the rest include the aerodynamic loads. Fig. 10 shows the corresponding variation of the calculated thrust and power coefficients.

The effect of single-step (SS) simulation, where the simulation stops at first iteration, and coupled-aero-structure (CAS) simulation, where the iterative process is converged when equilibrium between deformation and loading is achieved, was investigated and the result is illustrated in Fig 11. The slight effect on deformation is observed.

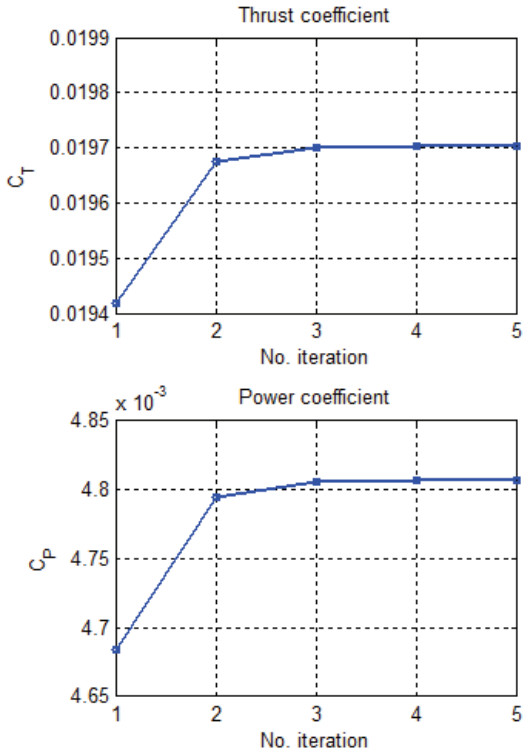

Figure 10. Variation of thrust coefficient during the iteration

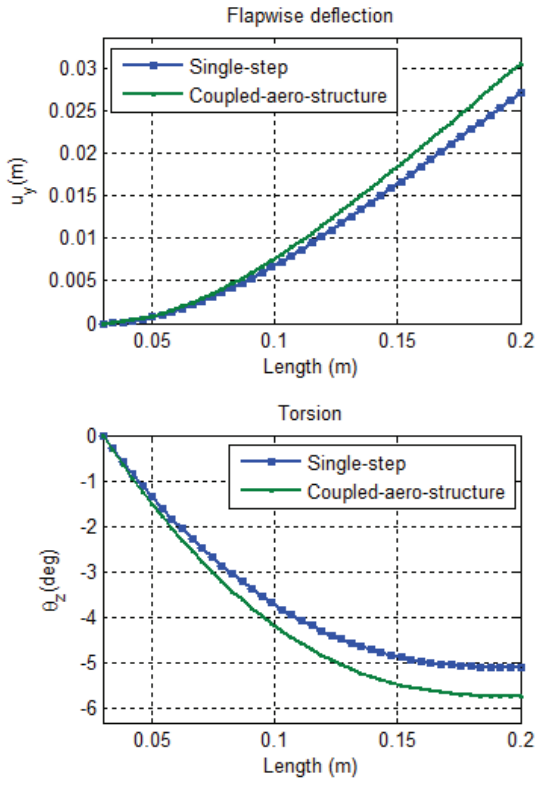

Figure 11. The effect of SS and CAS simulation on the blade deformations

3. EXPERIMENTAL SETUP

Optical measurement techniques have been developing for a couple of years in applications of aerodynamics, materials and structure, such as Holographic Interferometry (HI), Electronic Speckle Pattern Interferometry (ESPI), Projection Moiré Interferometry (PMI) and Digital Image Correlation (DIC) [11].

In 1998, Fleming G. A. obtained the 3-D deformation of rotor blade using PMI technique [12]. However, it has low sensitivity for in-plane deformation and moderate for out-of-plane deformation. By contrast, DIC has a relatively high sensitivity that can reach 1/30,000 of the test field [13].

In 2011, Lawson M. S. demonstrated the deformation of a rotating blade using DIC [14]. The technique was found to have many advantages including high resolution results, non-intrusive measurement, and good accuracy over a range of scales. However, DIC needs a preprocessing which is to apply a stochastic speckle pattern to the surface by spraying it with a high-contrast and non-reflective paint. This complex painting will probably affect the stiffness of blade. Hence, in this study, LDS was developed to measure blade deformation and validate the above numerical models. As is shown in Fig. 12, the two LDSs are driven by track systems to scan the blade from blade root to tip with an incremental distance 2mm.

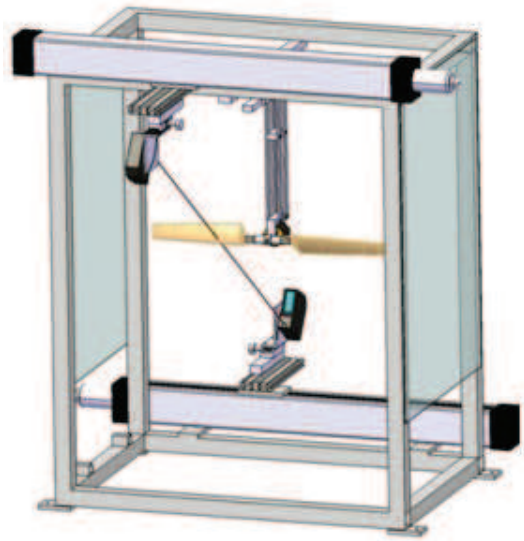

Figure 12. LDS rig

The LDS used in experiment is KEYENCE LK-G502. The distance of reference is 1000mm, and the range of measuring can be between -250mm to 500mm. The sampling frequency of this laser was selected as 10,000Hz. At each blade section, the laser scans for 2 seconds. Finally, 20,000 data points were obtained totally for each section.

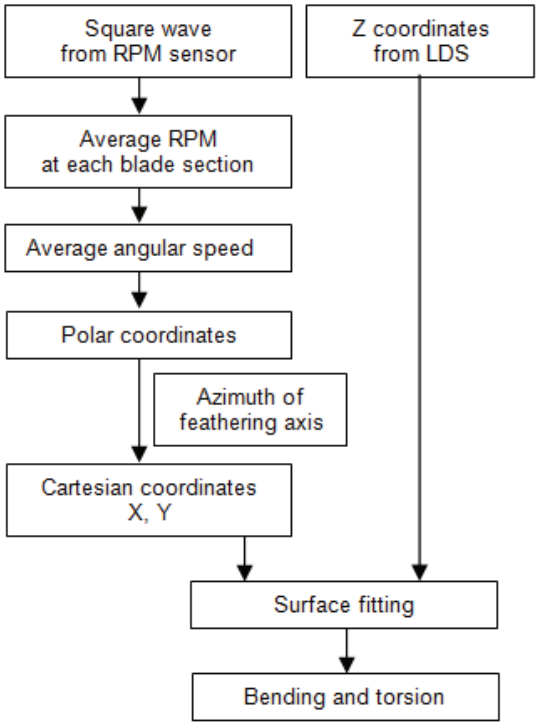

Figure 13. Post-processing procedure of LDS measuring

The post-processing of LDS measurement is shown in Fig. 13. Firstly, LDS records the Z coordinates which is the distance from the position detected on blade surface to reference plane. Meanwhile, square wave in time domain is measured by RPM sensor. Then, average RPM and angular speed at each blade section can be extracted from the square wave. Furthermore, with the azimuth of feathering, polar coordinates is possible to be transferred to Cartesian coordinates X and Y. Combining coordinates X, Y and Z, a polynomial surface fitting is performed to obtain the bending and torsion of rotating blade. Fig. 14 shows the surface fitting visualization of a deformed blade.

To evaluate the flexible blade performance, the thrust and torque were measured using two transducers. The close-up of mounted blade is shown in Fig 15.

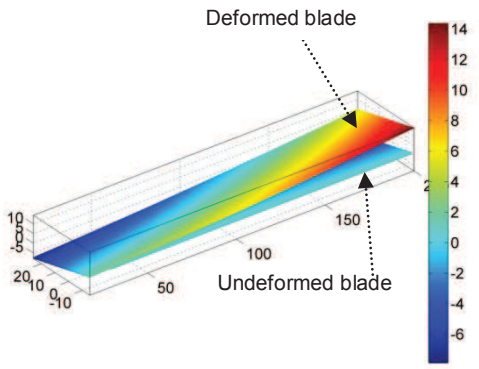

Figure 14. Surface fitting of a deformed blade

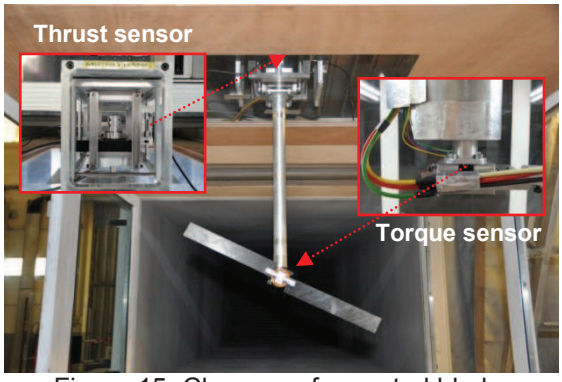

Figure 15. Close-up of mounted blade

Then, in order to evaluate the convergence of experimental data to the variation of sampling step, the standard deviation and average value were analyzed for both of thrust and torque. As we can see from Fig. 16, the deviations fluctuate when the sampling step is lower than 20,000. With increasing of sampling step, the deviations decrease and become relatively stable. By a compromise between data quality and time efficiency, the sampling step was determined as 60,000. The data convergence of torque was shown in Fig. 17. Sampling step 60,000 is also enough to obtain acceptable data of torque. Tests were operated two times to ensure the measuring stability. Acquisition precision is determined by Eq. 3.1 with 95% confidence intervals (factor t=1.96) [15].

$$U = \frac{t}{\sqrt{N}}\delta \tag{3.1}$$

where N is the total sampling number 60,000 in this study, δ is the standard deviation, and U is the precision of acquisition.

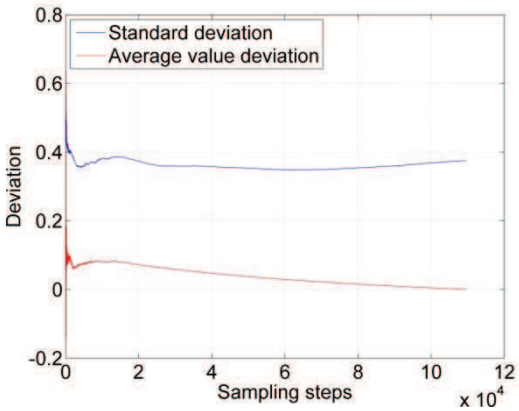

Figure 16. Convergence of thrust data

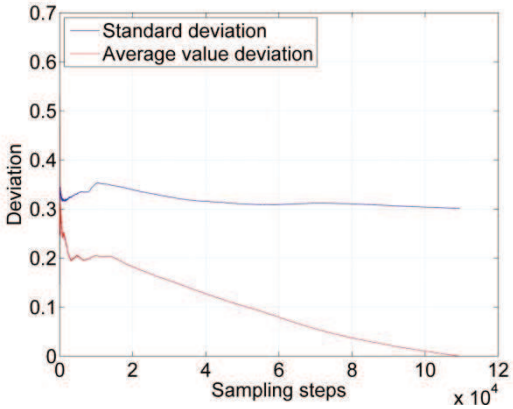

Figure 17. Convergence of torque data

4. RESULT VALIDATIONS

The validation results in performance are shown in Fig. 18. As can be seen, the FPROP agrees well with experimental data of thrust. However, it over-predicts the torque.

Fig. 19 shows the good agreement between the FAE simulation and the experimental data as obtained from LDS measurements. This is the result obtained for the blades clamped at collective pitch 35°. The fluctuations that can be observed through scattered plot of deformations are the results by the preliminary post-processing method. In this method, the deformation was extracted through the data interpolation at each section. Since the vibration of rotating blade probably generated uncertainty to the LDS data in spanwise, hence, the deformation exhibits unsmoothness in the plots.

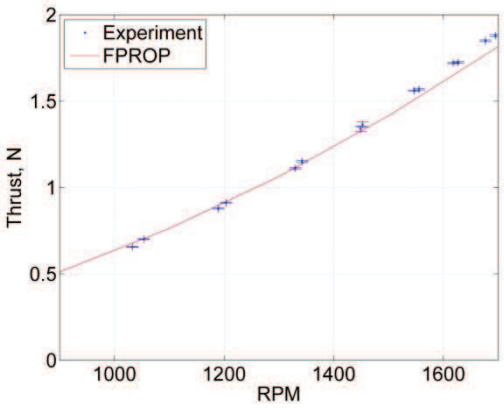

(a) Thrust

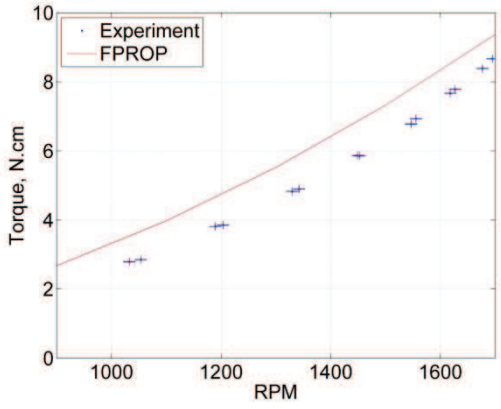

(b) Torque

Figure 18. Thrust and torque of rigid and flexible proprotor at different rotational speed (V=0)

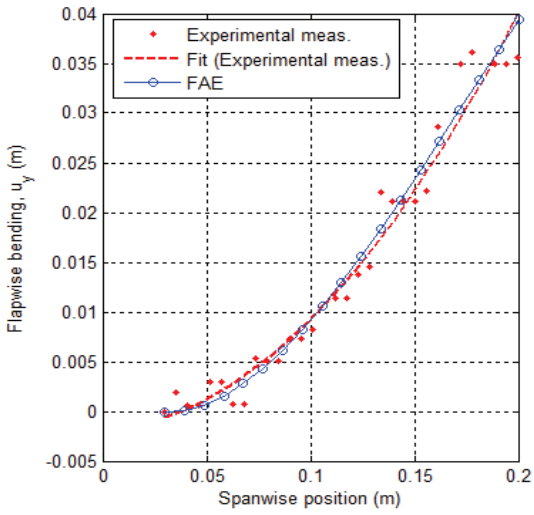

(a) Flapwise bending

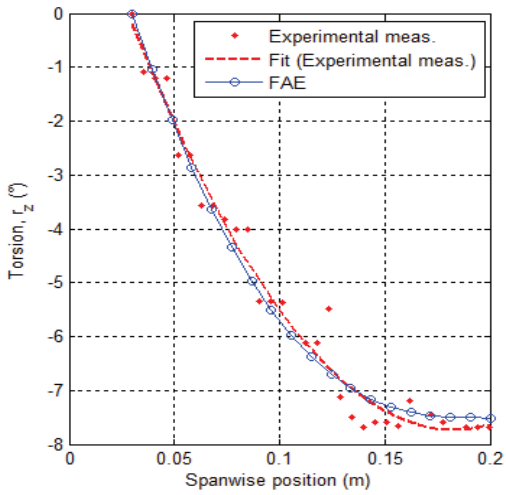

(b) Torsion

Figure 19. Comparison of FAE simulation with the corresponding measurements

5. CONCLUSIONS

As conclusion, the evaluation of design techniques, both for the aerodynamic performance and for the structural behavior of a composite flexible proprotor has been presented in rotor modes. The numerical model has capability of prediction in proprotor aerodynamics and structure. The model presents coupling between anisotropic beam finite element model and an aerodynamic model that takes into consideration the low Reynolds number aerodynamic. The influence of deformations is taken into account during the iteration procedure. The numerical model that utilizes the above-described approach has also been experimentally validated by LDS technique and transducers of thrust and torque. Through validation results of both aerodynamic and structural model, it can be concluded that the developed numerical model is valid as a reliable tool for designing and analyzing the proprotor made of composite material. Additionally, the developed structural model which uses cross-sectional analysis enables a more complex blade with highly-twisted and/or arbitrarily-shaped blades to be efficiently analyzed.

As perspectives, an investigation of static aeroelasticity on the UAV-sized flexible proprotor will be carried out using the validated numerical model. In future, the study will focus on propeller modes and optimization in composite laminates to enhance the proprotor efficiency. Likewise, based on inverse method, the loads on blade are expectedly able to be deducted from blade deformation.

6. REFERENCES

1. Shkarayev, S., Moschetta, J.M., Bataille, B., *Aerodynamic Design of Micro Air Vehicles for Vertical Flight*, Journal of Aircraft , vol. 45, no. 5, pp. 1715-1724, 2008

2. Nixon, M.W., *Improvements to Tilt Rotor PerformanceThrough Passive Blade Twist Control*, NASA Technical Memorandum 100583, 1-9, 1988.

3. Leishman, J., *Helicopter Aerodynamics. Cambridge*, 2nd edition, 2006.

4. Adkins, C.N., Liebeck, R.H., *Design of Optimum Propellers*, J. Propulsion and Power, 10, 676 – 682, 1990

5. Drela, M., *XFOIL: An Analysis and Design System for Low Reynolds Number Airfoil, Low Reynolds Number Aerodynamics*, Springer–Verlag, New York (1989) 1-12

6. Hein, B. R.,Chopra, I., *Hover Performance of a Micro Air Vehicle: Rotor at Low Reynolds number*, J. American Helicopter Society, 52 (2007) 254-262

7. Laitone, E.V., *Wind tunnel tests of wings at Reynolds numbers below 70,000*, Experiments in Fluids 23, pp405-409, Sringer-Verlag, 1997

8. Drela, M., *Elements of Airfoil Design Methodology in Applied Computational Aerodynamics*, (P. Henne, editor), AIAA Progress in Aeronautics and Astronautics, Volume 125, 1990

9. Blasques, J.P., Lazarov, B., *BECAS V2, A cross-section analysis tool for anisotropic and inhomogeneous beam sections of arbitrary geometry*," RisøTechnicalReportRisø-R 1785,TechnicalUniversity of Denmark, 2012

10. Kim, T., Branner, K., and Hansen, A. M, *Developing Anisotropic Beam Element for Design Composite Wind Turbine Blades*, In Proceedings of the 18th International Conference on Composite Material, Jeju, Korea, 21-26 August, 2011

11. Williams, D. C., *Optical Methods in Engineering Metrology*, Chapman and Hall, 1993

12. Fleming, G. A., Gorton S., *Measurement of Rotorcraft Blade Deformation Using Projection Moire Interferometry*, Proceedings of the Third International Conference on Vibration Measurements by Laser Techniques: Advances and Applications, SPIE--the International Society for Optical Engineering, Ancona, Italy, June 16-19, 1998, pp 514-527

13. Schmidt, T., Tyson, J., Galanulis, K., *Full-Field Dynamic Displacement and Strain Measurement Using Advanced 3D Image Correlation Photogrammetry: Part 1*, Experimental Techniques, 27(3), pp47-50, 2003

14. Michael, S., Lawson, Jayant, S., *Measurement of Deformation of Rotating Blades Using Digital Image Correlation*, 52nd AIAA/ASME/ASCE/AHS/ASC Structures, Structural Dynamics and Materials Conference April 2011, Denver, Colorado, AIAA 2011-1876, pp1-15

15. Thipyopas, C., Moschetta, J.M., *Experimental Analysis of a Fixed Wing VTOL. MAV in Ground* Effect, International Journal of Micro Air Vehicle, Vol. 2, no. 1, pp33-53